If we substitute the value of K from Eq. (13) into Eq. (12), the following expression for the terminal velocity of the bubble is obtained:

$$V_\infty = (-\sigma_T A)R_1\,[(R_2/R_1)^2 - 1]^2/(4\mu) \qquad (14)$$

With order-of-magnitude analysis, it may be shown from the results that the radial pressure gradient resulting from liquid acceleration near the ends of the slug is negligible compared to the axial pressure gradient in the liquid film when r_1 is sufficiently close to 1, for both small and large Reynolds numbers. Also, analysis of the normal stress balance at the interface reveals that the surface deformation is negligible if $(-\sigma_T)\,AL/\sigma \ll 1$, i.e., $\Delta\sigma/\sigma$ over the bubble surface is small compared to 1.

Equation (14) shows that the terminal velocity of the gas slug depends on $d\sigma/dT$, the viscosity of the liquid, the imposed temperature gradient, and the slug and tube radii, but is independent of the length of the slug. It is also interesting to note that the terminal velocity does not depend on the thermal diffusivity of the liquid, even though convective terms have been retained in the energy equation. This is because of the fully developed nature of the flow. Some representative values of the terminal velocity of a gas slug of radius 0.4 cm in a tube of radius 0.5 cm and subjected to a temperature gradient of 0.1°C/cm are 0.2 cm/s for liquid nitrogen, 0.07 cm/s for water, and 0.7 cm/s for lithium. The authors are not aware of any published results to compare the predicted values of the terminal velocity of the gas slug.

Conclusions

The steady-state motion of a large gas slug inside a tube filled with liquid and subjected to a linear temperature variation has been analyzed by taking into account the thermally induced gradient of the gas-liquid surface tension. An expression for the terminal velocity of the gas slug has been obtained.

References

[1]Young, N. O., Goldstein, J. S., and Block, M. J., "The Motion of Bubbles in a Vertical Temperature Gradient," *Journal of Fluid Mechanics,* Vol. 6, Oct. 1959, pp. 350–353.

[2]Thompson, R. L., "Marangoni Bubble Motion in Zero Gravity," NASA Tech. Memo. 79264, 1979.

[3]Balasubramaniam, R. and Chai, A. T., "Thermocapillary Migration of Droplets: An Exact Solution for Small Marangoni Numbers," *Journal of Colliod Interface Science,* Vol. 119, Oct. 1987, pp. 531–538.

Convective Heat Transfer with Multiflow in an Annular Pipe of Circular Cross Section

M. A. Ebadian*
Florida International University, Miami, Florida

A LITERATURE survey, including Kakac et al.,[1] Shah and London,[2] Soloukhin and Martynenko,[3] Eckert et al.,[4] Lundberg et al.,[5] Kays and Crawford,[6] Eckert and Drake,[7] Gebhart,[8] Bejan,[9] and Arpaci and Larsen,[10] indicates that convective heat transfer analysis for laminar flows in an annular circular conduit are traditionally based on lumped-parameter studies. The analysis presented herein of convective heat transfer in an annular circular tube subjected to a uniform outside wall temperature is based on actual velocity and temperature fields.

Fully developed laminar flows prevail over most of the flow length in highly compact heat exchangers that employ continuous flow passages geometries. Fully developed laminar flows also prevail in process heat exchangers that have highly viscous liquids as working fluids.

The exact temperature distribution for flows of an annular pipe subjected to a uniform wall heat flux was recently made available by Ebadian et al.[11] Using this distribution as a starting temperature field and employing the successive iteration method presented by Kays and Crawford,[6] Eckert and Drake,[7] Gebhar,[8] Bejan,[9] and Arpaci and Larsen,[10] the temperature fields in both flows are obtained analytically. Calculations were only carried out to the end of the first iteration. This is partly because of the increasing complexity of the calculations. However, even after one cycle of iterations, the values obtained for heat transfer characteristics corresponding to the limiting cases (simple circular pipe flow) are sufficiently close to classical values. For example, the Nusselt number for a circular section obtained after one iteration is 3.7288 compared to the exact value of 3.6568. One recent application of the successive iteration method is described in Ebadian et al.[12] where it was applied to the convective heat transfer problem of a single flow in an elliptic conduit and gave satisfactory results.

It was shown in Ebadian et al.[11] that the dimensionless heat transfer coefficients (Nusselt numbers) on the outer and inner separating surfaces of an annular circular pipe can be defined in three different ways (cases I, II, III, respectively). Since case I of Ebadian et al.[11] is most often applied in practical applications, only this case will be used in these calculations. According to this case, the heat transfer coefficients are based on the mixed flow bulk temperature of the inner and outer flows. The thickness and the thermal resistance of the inner separating wall are also neglected herein. The numerical results are given in graphical form. No experimental work was done and none is reported in the literature.

The importance of this work is in the design of heat exchangers. This information is necessary for designers as well as for the practitioner.

Temperature Fields

By neglecting the thermal resistance of the inner separation wall, and considering the secitons located sufficiently far from both entrances of the conduit where hydrodynamically and thermally fully developed flow conditions prevail, the continuity of temperature distribution is maintained by the forms

$$T_o = CZ + E_o(X,Y), \qquad T_i = CZ + E_{\text{in}} + E_i(X,Y) \qquad (1)$$

where T_o, T_i and E_o, E_i indicate the temperature and excess temperature distributions in outer and inner regions, respectively, for a constant heat flux condition. E_{in} represents the temperature at the inner separation surface for a constant heat flux case.

The continuity of the two temperature fields to be determined is satisfied by the following forms:

$$\bar{T}_o = \bar{E}_o(X,Y) \quad \text{and} \quad \bar{T}_i = \bar{E}_{\text{in}} + \bar{E}_i \qquad (2)$$

together with the boundary condition $\bar{T}_o = 0$ at the wall.

It must be noted that this selection cannot impose any restriction, and it can be used without any loss of generality of the problem. Therefore, the quantities $\bar{E}_o$, $\bar{E}_i$, and $\bar{E}_{\text{in}}$ represent cap temperatures in the outer and inner regions and at the separation surface, respectively.

Received Jan. 14, 1988; revision received April 18, 1987. Copyright © American Institute of Aeronautics and Astronautics, Inc., 1988. All rights reserved.

*Associate Professor, Department of Mechanical Engineering.

The energy equations to be satisfied in the inner and outer flow regions are

$$\frac{CZ - T_o}{CZ - T_m} CW_o = \frac{1}{R}\frac{\partial}{\partial R}\left(R\frac{\partial \bar{T}_o}{\partial R}\right) \tag{3a}$$

$$\frac{CZ - T_i}{CZ - T_m} CW_i = \frac{1}{R}\frac{\partial}{\partial R}\left(R\frac{\partial \bar{T}_i}{\partial R}\right) \tag{3b}$$

where T_m is the mixed mean temperature of the combined flow for constant heat flux (e.g., see Ref. 11).

The energy equations to be satisfied in each flow region expressed in dimensionless variables are,

$$ac(Pr)_o e_o w_o = \frac{1}{r}\frac{\partial}{\partial_r}\left(r\frac{\partial \bar{e}_o}{\partial r}\right) \qquad \text{for} \qquad \omega < r < 1 \tag{4a}$$

$$ac(Pr)_i(e_i + e_{\text{in}})w_i = \frac{1}{r}\frac{\partial}{\partial r}\left(r\frac{\partial \bar{e}_i}{\partial r}\right) \quad \text{for} \qquad o < r < \omega \tag{4b}$$

where

$$a = \frac{1 + k_c\lambda}{e_{\text{mo}} + k_c\lambda e_{\text{in}} + k_c\lambda e_{\text{mi}}} \tag{5}$$

and r is the dimensionless radial coordinate defined relative to the conduit radius L.

The boundary conditions for $\bar{e}_o$ and $\bar{e}_i$ are

$$\bar{e}_o = o, \quad \frac{d\bar{e}_i}{dr} = o \qquad \text{for} \qquad r = o \tag{6a}$$

$$\bar{e}_o = \bar{e}_{\text{in}}, \ \bar{e}_i = o \qquad \text{for} \qquad r = \omega \tag{6b}$$

where the functions e_o and e_i for constant heat flux are given in Ref. 8.

The solutions to Eq. (4) under the boundary conditions shown in Eq. (6) are determined by

$$\begin{aligned}\bar{e}_o = aG_o \Big\{ &\frac{e_{\text{in}}}{\ell n\omega}(B_1\,\ell n^2 r + B_2 r^2\,\ell nr + B_3\,\ell nr + B_4 r^2 + B_5)r^2 \\ &+ G_o[B_6 r^2\,\ell n^2 r + B_7\,\ell n^2 r + B_8 r^4\,\ell nr + B_9 r^2\,\ell nr \\ &+ B_{10}\,\ell nr + B_{11}r^6 + B_{12}r^4 + B_{13}r^2 + B_{14}]\,r^2 \\ &+ M_1\,\ell nr + N_1\Big\}\end{aligned} \tag{7a}$$

$$\begin{aligned}\bar{e}_i = aG_i\Big[&\frac{1}{16}\frac{e_{\text{in}}}{\omega^3}(4\omega^2 - r^2)r^2 - \frac{1}{16}\frac{G_i}{\omega^6}\left(\frac{3}{4}\omega^6 - \frac{7}{16}\omega^4 r^2\right. \\ &\left. + \frac{5}{36}\omega^2 r^4 - \frac{1}{64}r^6\right)r^2 + M_2\,\ell nr + N_2\Big]\end{aligned} \tag{7b}$$

where the factors B, M_1, N_1, M_2, N_2 are calculated explicitly in terms of ω.

Heat transfer continuity on the inner separating surface is satisfied by the relation

$$k_o\left(\frac{\partial \bar{e}_o}{\partial r}\right)_{r=\omega} = k_i\left(\frac{\partial \bar{e}_i}{\partial r}\right)_{r=\omega} \tag{8}$$

This condition, after introducing an alternate dimensionless temperature on the separating surface as $\bar{\beta} = \bar{e}_{\text{in}}\,G_o$, will yield

$$\begin{aligned}\bar{\beta} = -a\omega G_o\Big[&\beta\left(C_1\,\ell n^2\omega + C_2\,\ell n\omega + C_3\frac{1}{\ell n\omega} + C_4\right) \\ &+ C_5\,\ell n^3\omega + C_6\,\ell n^2\omega + C_7\,\ell n\omega + C_8 \\ &+ \frac{1}{16}\left(4\beta\omega^3 - \frac{\eta}{k_k}C_9\right)\eta\,\ell n\omega\Big]\end{aligned} \tag{9}$$

where the factors C are calculated explicitly in terms of ω.

Heat Fluxes and Heat Transfer Coefficients

The rate of heat flow per unit length of conduit, through the outer and inner surfaces, considered positive when flowing into the outer region, is expressed, respectively, as [e.g., see Ref. (13)]:

$$U_o = 2\pi LF\left(\frac{\partial \bar{e}_o}{\partial r}\right)_{r=1}, \qquad U_i = 2\pi\omega LF\left(\frac{\partial \bar{e}_o}{\partial r}\right)_{r=\omega} \tag{10}$$

Substituting $\bar{e}_o$ and $\bar{e}_i$ from Eq. (7), one obtains

$$U_o = 2\pi LFG_o\left[aG_o\left(\frac{\beta}{\ell n\omega}D_1 + D_2\right) + \frac{\bar{\beta}}{\ell n\omega}\right] \tag{11a}$$

$$U_i = -2\pi LF\omega G_o\left[aG_o\left(\frac{\beta}{\ell n\omega}E_1 + E_2\right) + \frac{\bar{\beta}}{\omega\,\ell n\omega}\right] \tag{11b}$$

where factors D and E are calculated explicitly in terms of ω.

The Nusselt numbers herein are defined using the definition given in Ebadian et al.,[11] for case I where the inner and outer wall heat transfer coefficients are based on the mixed flow bulk temperature is expressed as

$$\begin{aligned}\bar{T}_m = &\frac{1}{C_{po}Q_o + C_{pi}Q_i} \\ &\times\left(C_{po}\rho_o\int_{A_o} W_o\bar{T}_o\,dA + C_{pi}\rho_i\int_{A_i} W_i\bar{T}_i\,dA\right)\end{aligned} \tag{12}$$

where C_{po}, A_o and C_{pi}, A_i are the specific heat and cross-sectional area for the outer and inner passages, respectively.

The heat transfer coefficients on the outer wall and on the inner separating surface ($\bar{h}_o$, $\bar{h}_i$) are calculated from

$$\begin{aligned}U_o &= (\bar{T}_{\text{wall}} - \bar{T}_m)\,2\pi L\bar{h}_o, \\ U_i &= (\bar{T}_{\text{wall}} + \bar{E}_{\text{in}} - \bar{T}_m)\,2\pi\omega L\bar{h}_i\end{aligned} \tag{13}$$

where $\bar{T}_{\text{wall}} = 0$.

Selecting the fluid in the outer passage as the reference fluid, the dimensionless heat transfer coefficient (the Nusselt numbers) on each surface based on their respective diameters are defined by

$$(Nu)_o = (2L/k_o)\bar{h}_o \qquad \text{and} \qquad (Nu)_i = (2\omega L/k_o)\bar{h}_i \tag{14}$$

The expression for a in Eq. (5) can be changed into the form

$$aG_o = \frac{I_{oo} + \frac{1}{4}\eta\omega^4}{-(J_o/G_o) + \frac{1}{4}\eta\omega^4\beta - \beta(J_i/G_o)} \tag{15}$$

Equating the heat flow expressions in Eq. (11) and Eq. (13), and simplifying, gives

$$\begin{aligned}&aG_o\left(D_1\frac{\beta}{\ell n\omega} + D_2\right) + \frac{\bar{\beta}}{\ell n\omega} \\ &= \frac{1}{2}\frac{(\bar{J}_o/G_o) + \eta(\bar{J}_i/G_o) - \frac{1}{4}\eta\omega^4\bar{\beta}}{I_{oo} + \frac{1}{4}\eta\omega^4}(Nu)_o\end{aligned} \tag{16a}$$

$$\begin{aligned}&aG_o\left(E_1\frac{\beta}{\ell n\omega} + E_2\right)\omega + \frac{\bar{\beta}}{\ell n\omega} \\ &= \frac{1}{2}\frac{(\bar{J}_o/G_o) + \eta(\bar{J}_i/G_o) + \beta\bar{I}_{oo}}{I_{oo} + \frac{1}{4}\eta\omega^4}(Nu)_i\end{aligned} \tag{16b}$$

An inspection of the expressions for $(Nu)_o$ and $(Nu)_i$ reveals that the Nusselt number for an annular pipe maintained under a constant wall temperature, besides the geometric factor ω, depends on the following parameters:

1) The ratio of the thermal conductivity of the fluid within the inner and outer passages (k_k).

2) The product k_k and the ratio of the Peclet numbers k_{pe} for the flows within the inner and outer passages ($\eta = k_k\, k_{pe}$, the heat exchange number of an annular pipe).

Results and Discussion

Selecting a value for the ratio of the thermal conductivity of two fluids to be $k_k = 1$, and using four values (1, 10, -1, -10) for the dimensionless heat exchange number η, the Nusselt numbers are plotted against the dimensionless radius of the separating surface. The resulting curves are presented in Figs. 1 and 2. In order to compare these results with the case of constant wall heat flux conditions, the ratio of the Nusselt numbers for constant heat flux to those for constant wall temperature are also plotted against the dimensionless radius of the separating surface while using the same numerical factors used above. These results are presented in Figs. 3 and 4.

Figure 1

These curves show the variation in the outer wall Nusselt number $(Nu)_o$ as a function of the dimensionless radius (ω) of the separating surface for four values of the heat exchange number η (i.e., 1, 10, -1, -10) corresponding to parallel and counterflow arrangements. It can be observed that in the limiting cases of $\omega = 0$ and $\omega = 1$, the system reduces to a simple pipe having a single flow maintained under constant wall temperature. The value of the Nusselt number obtained for this case is 3.7288, which is not exactly the same as the classical value of 3.6568. The reason is that, in this analysis, the calculations are only carried through the first approximation. The curves show that the outer wall Nusselt number for an annular tube with $\eta = 1.0$ has a larger value than that of a simple pipe when ω is between 0.0 and 0.5417, and has a smaller value than that of a simple pipe, when ω is between 0.5417 and 1.0. For an annular tube with $\eta = 10.0$, the same behavior holds, except the transition occurs at a smaller value of $\omega = 0.3220$. In case of counterflow arrangements with $\eta = -1.0$ and $\eta = -10.0$, curves have vertical asymptotes at $\omega = 0.4745$ and $\omega = 0.3348$, respectively. These points correspond to the special cases for which the bulk temperature of the combined flow of the counterflow arrangements vanishes.

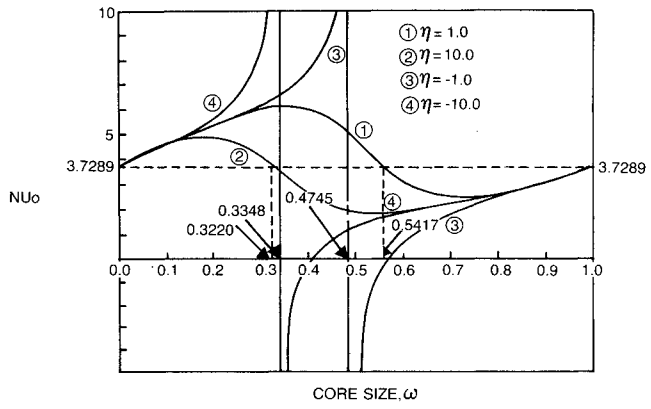

Fig. 1 Outer Nusselt number vs the core size.

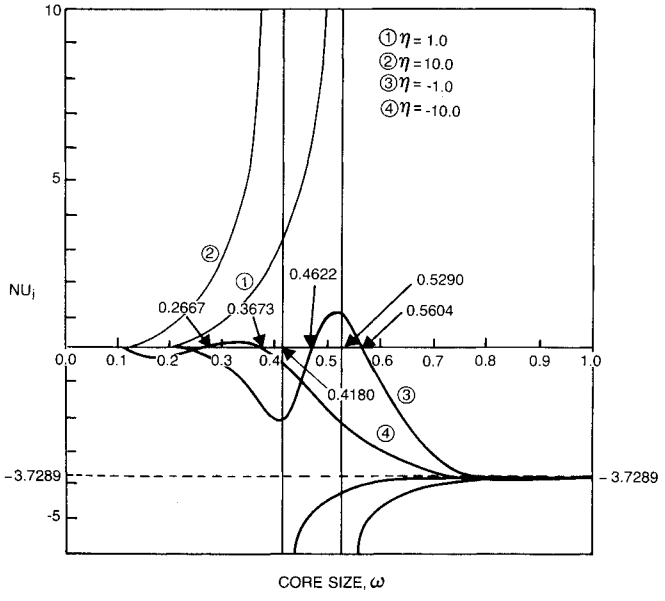

Fig. 2 Inner Nusselt number vs the core size.

Figure 2

These curves show the variation of the inner Nusselt number $(Nu)_i$ of the inner separation surface with the dimensionless radius (ω), for four values of heat exchange number η (i.e., 1, 10, -1, -10), corresponding to parallel and counterflow arrangements. One can observe that for the limiting case of $\omega = 1.0$, the system reduces to a simple pipe and the Nusselt number approaches a value of 3.7288, whose significance has already been discussed. For the other limiting case of $\omega = 0$, the internal surface disappears and consequently, the dimensionless heat transfer coefficient becomes zero. In case of a parallel flow arrangement, both curves have vertical asymptotes at $\omega = 0.5290$ and $\omega = 0.4180$, respectively. The physical significance of these special points is that for these ω values, the bulk temperature of the combined flow becomes equal to the temperature of the inner separating wall. In case of a counterflow arrangement, one can observe that for $\eta = -10.0$, the Nusselt number has positive values when $0.2667 \le \omega \le 0.3673$. This corresponds to a situation where the heat

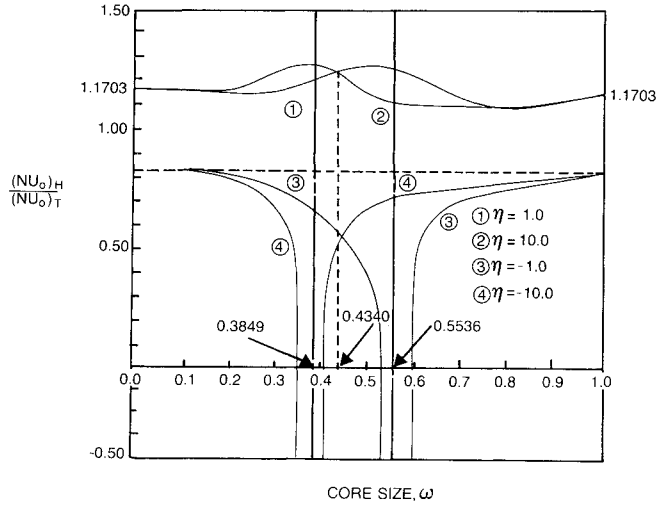

Fig. 3 Ratio of outer Nusselt number with constant wall heat flux to constant wall temperature.

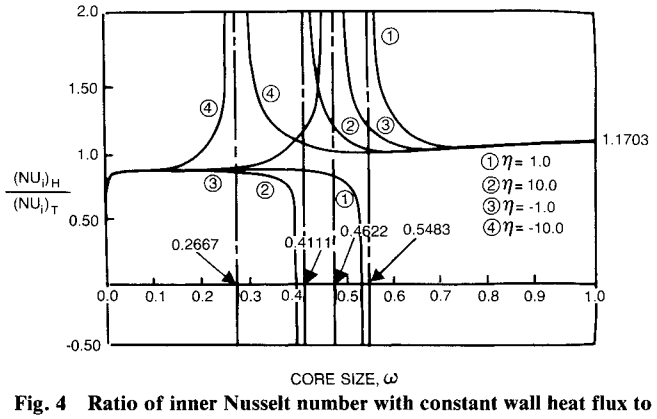

Fig. 4 Ratio of inner Nusselt number with constant wall heat flux to constant wall temperature.

transfer through the separation wall is taking place from inner to outer flow. For all other values of ω, the heat transfer direction at the separation surface is from outer to inner flow. The curve for $\eta = -1.0$ displays a similar behavior, with the difference being that the ω interval shifts to a new position of $0.4622 \leq \omega \leq 0.5604$.

Figure 3

These curves show the variation of the ratio of the Nusselt numbers for constant heat flux $(Nu_o)_H$ to the Nusselt number for constant wall temperature $(Nu_o)_T$, for four values of heat exchanger number η (i.e., 1, 10, -1, -10), corresponding to parallel and counterflow arrangements. It can be observed that for parallel flow arrangements this ratio is always greater than one. In the limiting cases of $\omega = 0$ and $\omega = 1.0$, corresponding to the case of a simple pipe, the ratio obtained has a value of 1.1703. The classical value of this ratio is 1.1930. This discrepancy is attributed to the fact that the analysis presented herein includes only the first approximation from the "iteration method" used. Moreover, there is a particular value of ω for parallel flow arrangement (i.e., $\omega = 0.4340$) for which a phenomenon occurs. When the core size is smaller than this number, the ratio of the Nusselt numbers for $\eta = 1.0$ is smaller than the ratio of the Nusselt numbers for $\eta = 10.0$. When the core size is greater than 0.4340, the opposite phenomenon occurs. In case of a counterflow arrangement, the curve with $\eta = 1.0$ has one vertical asymptote at $\omega = 0.5536$, and the curve with $\eta = -10.0$ has another vertical asymptote at $\omega = 0.3849$. The physical significance of these asymptotes is such that they correspond to ω values of Fig. 1 for which $(Nu)_o$ vanishes.

Figure 4

These curves show the variation of the ratio of the inner Nusselt number for constant heat flux $(Nu_i)_H$ to constant wall temperature $(Nu_i)_T$ for four values of heat exchanger number η (i.e., 1, 10, -1, -10), corresponding to parallel and counterflow arrangements. As in the previous limiting case of $\omega = 1.0$, the ratio has the same value of 1.1703 representing the simple flow situation. However, in the limiting case of $\omega = 0$, the ratio is approaching a value of zero. The curve with $\eta = 1.0$ has an asymptote at $\omega = 0.5483$, and the curve with $\eta = 10.0$ has a asymptote at $\omega = 0.4111$. The meaning of this behavior is that, at some values of ω, these curves are crossing the horizontal axis. That is, at these ω values, the heat transfer at the separating surface is changing its direction. Moreover, for both cases where $\eta = 1.0$ and $\eta = 10.0$, the ratio has an optimum value of 0.85 at $\omega = 0.0350$. In case of counterflow arrangements, the curve with $\eta = -10.0$ has an asymptote at $\omega = 0.2667$ and the curve with $\eta = -1.0$ has an asymptote at $\omega = 0.4622$.

Acknowledgment

This material is based upon work supported by the National Science Foundation under Grant R11-8305297.

References

[1]Kakac, S., Shah, R. K., and Aung, W., *Handbook of Single Phase Convective Heat Transfer*, Wiley-Interscience, New York, 1987.

[2]Shah, R. K. and London, A. L., *Laminar Flow Forced Convection in Ducts*, Academic, New York, 1978.

[3]Soloukhin, R. I. and Martynenko, O. G., "Heat and Mass Transfer Bibliography-Soviet Literature," *International Journal of Heat and Mass Transfer*, Vol. 26, 1983, pp. 1771-1781.

[4]Eckert, E. R. G., Goldstein, R. J., Pfender, E. Ibele, W. E., Patanker, S. W., Ramsey, S. W., Simon, T. W., Deckor, N. A., Kuehn, T. H., Lee, H. O., and Girshick, S. L., "Heat Transfer – A Review of the 1985 Literature," *International Journal of Heat and Mass Transfer*, Vol. 29, 1986, pp. 1767-1842.

[5]Lundberg, R. E., Reynolds, W. C., and Kays, W. M., "Heat Transfer with Laminar Flow in Concentric Annuli with Constant and Variable Wall Temperature with Heat Flux," NASA TN D-1972, Aug. 1963.

[6]Kays, W. M. and Crawford, M. E., *Convective Heat and Mass Transfer*, McGraw-Hill, New York, 1980.

[7]Eckert, E. R. G. and Drake, R. M., Jr., *Analysis of Heat and Mass Transfer*, McGraw-Hill, New York, 1972.

[8]Gebhart, B., *Heat Transfer*, McGraw-Hill, New York, 1971.

[9]Bejan, A., *Convective Heat Transfer*, Wiley-Interscience, New York, 1984.

[10]Arpaci, V. S. and Larsen, P. S., *Convective Heat Transfer*, Prentice-Hall, Englewood Cliffs, NJ, 1984.

[11]Ebadian, M. A., Topakoglu, H. C., and Arnas, O. A., "Convective Heat Transfer for Laminar Flows in a Multi-Passage Circular Pipe Subjected to an External Uniform Heat Flux," *International Journal of Heat and Mass Transfer*, Vol. 29, 1986, pp. 107-117.

[12]Ebadian, M. A., Topakoglu, H. C., and Arnas, O. A., "On the Convective Heat Transfer in a Tube of Elliptic Cross-Section Maintained Under Constant Wall Temperature," *Journal of Heat Transfer*, Vol. 106, 1986, pp. 33-39.

[13]Topakoglu, H. C. and Arnas, O. A., "Convective Heat Transfer for Steady Laminar Flow Between Two Confocal Elliptic Pipes with Longitudinal Uniform Wall Temperature Gradient," *International Journal of Heat and Mass Transfer*, Vol. 17, 1974, pp. 1978-1988.

Friction Coefficients for Flow in Pipes with Mass Injection and Extraction

Jerry Bowman*
U.S. Air Force Academy, Colorado Springs, Colorado
and
James Hitchcock†
Air Force Institute of Technology, Dayton, Ohio

Theme

FUNCTIONS for friction coefficients are presented for flow in a pipe with mass injection or extraction. The expressions are valid for compressible flows (Mach numbers as high as 1) with very large mass injection or extraction rates (radial Reynolds numbers up to 20,000). In order to develop these relationships, a porous pipe with air injection and extraction was studied experimentally and numerically. For the numerical model, the compressible, axisymmetric, Navier-Stokes equations were solved using MacCormack's explicit finite-difference method. No boundary-layer assumptions were made. Experimentally, pressure variations axially and velocity variations axially and radially inside the porous pipe were measured. The experimental data were used to show that numerical solutions gave valid results. Friction coefficient expressions were developed using the numerical data. They were shown to give excellent results when used in a one-dimensional model to predict compressible flow dynamics resulting from mass injection/extraction.

Contents

Figure 1 is a representation of the system studied experimentally and numerically. During the experiment a high-pressure air source (6.9×10^5 N/m^2 gage) provided air that was injected radially into a porous pipe. The air would then flow axially down the pipe and exit radially through a second section of

Presented as Paper 87-0657 at the AIAA 26th Aerospace Sciences Meeting, Reno, NV, Jan. 12-15, 1987; received Dec. 21, 1987; revision received June 17, 1988. This paper is declared a work of the U.S. Government and is not subject to copyright protection in the United States.

*Assistant Professor, Aeronautical Engineering Department.
†Professor, Department of Aeronautics and Astronautics.